THE JOURNAL OF BIOLOGICAL CHEMISTRY VOL. 285, NO. 13, pp. 9868–9880, March 26, 2010

Low Density Subcellular Fractions Enhance Disease-specific Prion Protein Misfolding[S]

Received for publication, December 11, 2009, and in revised form, January 20, 2010 Published, JBC Papers in Press, January 27, 2010, DOI 10.1074/jbc.M109.093484

James F. Graham[‡1], **Sonya Agarwal**[‡2], **Dominic Kurian**[§], **Louise Kirby**[‡3], **Teresa J. T. Pinheiro**[¶], **and Andrew C. Gill**[‡2,4]

From the [‡]*Neuropathogenesis Division, The Roslin Institute and Royal (Dick) School of Veterinary Studies, University of Edinburgh, Alexander Robertson Building, Easter Bush Veterinary Centre, Roslin, Midlothian EH25 9RG, the* [§]*Institute for Animal Health, Compton, Newbury, Berkshire RG20 7NN, and the* [¶]*School of Biological Sciences, University of Warwick, Gibbet Hill Road, Coventry CV4 7AL, United Kingdom*

The production of prion particles *in vitro* by amplification with or without exogenous seed typically results in infectivity titers less than those associated with PrP^{Sc} isolated *ex vivo* and highlights the potential role of co-factors that can catalyze disease-specific prion protein misfolding *in vivo*. We used a cell-free conversion assay previously shown to replicate many aspects of transmissible spongiform encephalopathy disease to investigate the cellular location of disease-specific co-factors using fractions derived from gradient centrifugation of a scrapie-susceptible cell line. Fractions from the low density region of the gradient doubled the efficiency of conversion of recombinant PrP. These fractions contain plasma membrane and cytoplasmic proteins, and conversion enhancement can be achieved using PrP^{Sc} derived from two different strains of mouse-passaged scrapie as seed. Equivalent fractions from a second scrapie-susceptible cell line also stimulate conversion. We also show that subcellular fractions enhancing disease-specific prion protein conversion prevent *in vitro* fibrillization of recombinant prion protein, suggesting the existence of separate, competing mechanisms of disease-specific and nonspecific misfolding *in vivo*.

The transmissible spongiform encephalopathies (TSEs)[5] are a family of neurodegenerative disorders that cause disease in a wide range of host species. TSEs include scrapie in sheep and goats, bovine spongiform encephalopathy (BSE) in cattle, chronic wasting disease in cervids, and different forms of disease in humans, including variant Creutzfeldt-Jakob disease. There is also evidence for the transmission of TSEs to various captive animal species, presumably through the consumption of BSE-infected meat. TSEs have a prolonged incubation period of many months, and clinical signs include pruritis, ataxia, and dementia leading invariably to death. The principle pathological manifestations include astrocytic gliosis, neuronal loss, and spongiform degeneration. In most TSEs there is also deposition of an aggregated and misfolded form of a normal cellular host protein, PrP^{C}, or the prion protein. During TSEs, also termed prion diseases, the prion protein misfolds into an alternate isoform, PrP^{Sc}, which is composed predominately of the β-sheet and is partially protease-resistant. It is widely believed that the disease-associated isoform, PrP^{Sc}, represents the infectious agent of TSE diseases and is capable of using its structure as a template for endogenous PrP^{C} molecules after inoculation or ingestion of PrP^{Sc}-containing preparations (1). This hypothesis has been considerably strengthened through recent reports of the *in vitro* generation of misfolded isoforms of either tissue homogenate-derived or recombinant prion protein (recPrP) that appear to cause TSE disease on inoculation into suitable hosts (2–6).

A variety of different TSE strains exist that cause diseases with distinctive pathology, clinical signs, and/or incubation times in the same host. It is widely believed that these strains are encoded by different PrP^{Sc} conformations, which requires a plethora of stable conformations to exist concomitantly (7, 8). To account for this, it has been suggested that prion co-factors exist that participate in misfolding of PrP^{C} to generate PrP^{Sc} of strain-specific conformations (8–10). Additionally, i*n vitro* misfolding assays that have been reported to generate *de novo* infectivity almost exclusively use PrP^{C}-enriched from or contained within tissue homogenates (2, 6), whereas those assays that use purified recPrP do not appear to generate infectivity (11, 12) or at least not to levels allowing efficient infections of wild type animals (3, 4, 13). These observations strongly suggest the presence of additional factors in tissue homogenates that facilitate prion misfolding to genuine disease-specific isoforms.

A recent study by Deleault *et al.* (14) identified a minimal set of molecules that can be added to PrP^{C} purified from brain homogenate to create conditions that will generate *de novo* TSE infectivity. The PrP^{C} co-purified with various lipidic components and this substrate along with exogenously added poly(A)RNA (which appears crucial) not only supported amplification of proteinase K (PK)-resistant protein when seeded

[S] The on-line version of this article (available at http://www.jbc.org) contains supplemental "Materials and Methods," Figs. S1–S6, and Table I.

[1] Supported by a doctoral training account from the Biotechnology and Biological Sciences Research Council, Swindon, United Kingdom.
[2] Supported through an Institute Strategic Programme Grant from the Biotechnology and Biological Sciences Research Council, Swindon, United Kingdom.
[3] Supported by the Department for Environment, Food, and Rural Affairs.
[4] To whom correspondence should be addressed. Tel.: 44-131-6517310; Fax: 131-4400434; E-mail: andrew.gill@roslin.ed.ac.uk.

[5] The abbreviations used are: TSE, transmissible spongiform encephalopathy; BSE, bovine spongiform encephalopathy; CFCA, cell free conversion assay; MS, mass spectrometry; PK, proteinase K; PMCA, protein misfolding cyclic amplification; PrP^{C}, cellular prion protein; PrP^{Sc}, scrapie-associated prion protein; recPrP, recombinant PrP; SMB-PS, scrapie mouse brain cells cured of scrapie by treatment with pentosan polysulfate; ThT, thioflavin T; Δ3F4-recPrP, recombinant PrP incorporating the 3F4 antibody recognition motif; Bis-Tris, 2-[bis(2-hydroxyethyl)amino]-2-(hydroxymethyl)propane-1,3-diol; MES, 2-*N*-morpholino)ethanesulfonic acid; ER, endoplasmic reticulum; HPLC, high performance liquid chromatography.

with PrP^{Sc} but also appeared to generate PK-resistant protein in the absence of a seed. The *in vitro* misfolding assay used was based upon the protein misfolding cyclic amplification (PMCA) assay, which involves serial rounds of sonication, thereby imparting a significant amount of energy into the prion misfolding system. From these experiments, it cannot be ruled out that additional, as yet undefined components also co-purified with the PrP^{C} from uninfected brains or that the sonication involved in PMCA conditions creates the energy needed to replace additional co-factors that may be absent from this assay but are required *in vivo*.

To address these possibilities, we have begun a series of investigations by use of a traditional cell-free conversion assay (CFCA) in which external sources of energy (sonication or shaking) are omitted (15, 16). We have also used bacterially derived recombinant PrP as a substrate, and this assay, although producing low yields of newly formed PK-resistant recombinant PrP, represents a well defined system in which we know that alterations in conversion efficiency are the result of factors within our control. In the current study we have used our CFCA to investigate whether a scrapie-susceptible, fibroblastic cell line, LD9 (17), contains co-factors capable of enhancing PrP misfolding. We performed subcellular fractionation of the cells and found that low density cellular components stimulated conversion of recombinant PrP seeded with PrP^{Sc} derived from ME7-infected mouse brains. These fractions were composed of both plasma membrane and cytoplasmic proteins, and we further showed that the same preparations enhanced prion protein conversion seeded by an alternate strain of scrapie, 79A. Similar fractions derived from an alternate scrapie-susceptible cell line, SMB-PS, also stimulated our ME7-seeded CFCA. Finally, we also showed that low density fractions prevent fibrillization of recombinant PrP in unseeded *in vitro* assays, suggesting that disease-specific and generic misfolding pathways may represent differing, competing pathways of prion protein misfolding *in vivo*.

EXPERIMENTAL PROCEDURES

Culture of LD9 and SMB Cells—LD9 cells were a kind gift from Prof. Charles Weissmann (Scripps, Florida). SMB-PS cells were obtained from the TSE Resource Centre, Institute for Animal Health, Compton, UK. All tissue cultures were maintained in a Hera Cell 240 incubator (Heraeus) at 37 °C and 5% CO_2 in 75-ml flasks. LD9 cells were maintained in Eagle's minimal essential media (Invitrogen) supplemented with 10% (v/v) fetal calf serum. SMB-PS cells were maintained in Media 199 supplemented with 5% (v/v) fetal calf serum and 10% (v/v) Hanks' buffered salt solution. Cells were split when they had achieved 90% confluency, as judged by light microscopy, by treating with trypsin solution (Invitrogen) for 5 min to detach cells.

Subcellular Fractionation—Before fractionation, cells washed with phosphate-buffered saline and the contents of a T75 flask were mechanically lysed in 10 ml of homogenization buffer (250 mM sucrose, 1 mM EDTA, 20 mM HEPES, pH 7.4, containing EDTA-free complete protease inhibitors (Roche Applied Science)) by 10 strokes of a Dounce homogenizer. The homogenate was centrifuged briefly (10 min, 1000 × *g*) to clear nuclei and cellular debris to create a post-nuclear supernatant, which was used for fractionation. 10-ml gradients of 10–20% OptiPrep were made in Beckman Ultraclear tubes (14 × 89 mm) by sequentially placing 2-ml volumes of 20, 17.5, 15, 12.5, and 10% OptiPrep solutions carefully on top of each other. The discontinuous gradient was incubated at 4 °C for 12 h to form a continuous gradient. A protein assay was performed on post-nuclear supernatant by use of a 2D quant kit (Amersham Biosciences), and a volume equivalent to 1.5 mg of protein (~1 ml) was layered on top of each continuous OptiPrep gradient. The tubes were centrifuged for 8 h at 228,000 × *g* in a TH-641 rotor (Sorvall). After centrifugation, 500-μl fractions were removed from the top of the tube to yield 22 subcellular fractions per tube. The proteins contained in each fraction were precipitated by the addition of 1 ml of ice-cold methanol for 12 h, and the pellets were stored at −80 °C before use.

Purification of Scrapie-associated Fibrils—The method for isolation of scrapie-associated fibrils has previously been published (18) and is based around detergent extraction and differential centrifugation. More details can be found in the supplemental Materials and Methods.

Production of Murine Wild type and Δ3F4 Recombinant PrP—We have previously published details of the basic expression and purification procedures applied to bacterial-expressed, wild type, murine recombinant PrP (19). A construct for Δ3F4-recPrP was generated by introducing the mutations L108M and V111M by site-directed mutagenesis (QuikChange, Stratagene). More details of the purification strategy adopted are contained within supplemental Materials and Methods, but recPrP was isolated from bacteria by lysis with lysozyme, inclusion bodies were solubilized in a urea containing buffer, and recPrP was purified by metal ion affinity chromatography and cation exchange chromatography. Purified protein was oxidized and then dialyzed extensively against sodium acetate. Final protein solutions were concentrated to ~1 mg/ml and stored at −80 °C before use.

Cell-free Conversion Assays—Details of our CFCA procedure have previously been published (15), and more details can be found in the supplemental Materials and Methods. In the current experiments we supplemented our standard cell-free conversion assay with fractions derived from subcellular fractionation and treated the assay as normal. CFCA conversion efficiencies were tested for deviations from control reactions by one-sample *t* tests and were deemed significant if $p < 0.05$.

SDS-PAGE and Western Blotting—The NuPAGE system (Invitrogen) was used for all SDS-PAGE separations. Samples for analysis were diluted 3:1 with 4× LDS sample buffer and heated for 10 min in a boiling water bath. Proteins were resolved on pre-cast 12% Bis-Tris NuPAGE gels (Invitrogen), and 5 μl of SeeBlue Plus was used as the molecular weight standard. Pre-cast gels were electrophoresed at 170 V for approximately 1 h and were either visualized by Coomassie Brilliant Blue or silver staining or used for Western blotting.

SDS-PAGE gels were blotted to polyvinylidene difluoride membranes (Millipore) by use of a semidry blotter (Invitrogen) for 1 h 30 min at 100 mA. The membrane was blocked for 1 h at room temperature in 5% Marvel solution and probed with either 3F4 anti-PrP monoclonal antibody (TSE Resource Centre) or antibodies specific to chosen subcellular marker pro-

teins. Goat anti-mouse secondary antibody coupled to horseradish peroxidase was used, and the signal was developed by ECL (GE Healthcare). Gel images were captured by use of a Image Master III scanner (GE Healthcare), and densitometric analysis was performed by use of ImageQuant software (GE Healthcare).

HPLC-MS/MS—Before LC-MS/MS analysis, proteins were reduced, alkylated, and digested with trypsin according to previously published methods (20). LC MS/MS analysis was performed by use of a nanoAcquity ultra performance liquid chromatography system coupled to quadrupole-time of flight Premier mass spectrometer (Waters Corp.) at the proteomics facility of the Institute for Animal Health. Tryptic peptides were desalted and concentrated on a C18 trap (180 μm × 20 mm, 5-μm symmetry, Waters) for 3 min at 10 μl/min with 0.1% (v/v) formic acid and resolved on a 1.7-μm BEH 130 C18 column (100 μm × 100 mm, Waters). Peptides were eluted at 400 nl/min with a linear gradient of 0–50% (v/v) acetonitrile with 0.1% (v/v) formic acid over 30 min followed by 85% (v/v) acetonitrile with 0.1% (v/v) formic acid for 7 min. Eluted peptides were analyzed on a quadrupole-time of flight mass spectrometer in data-directed acquisition mode, where a MS survey scan was used to automatically select multicharged peptides for further MS/MS fragmentation. From each survey scan up to three peptides were selected for fragmentation. MS/MS collision energy was dependent on precursor ion mass and charge state. A reference spectrum was collected at every 30 s from the Glu-fibrinopeptide B (785.8426 m/z), introduced via a reference sprayer. Two discrete analyses were performed, the second of which included an exclusion list of all the peptides identified in the first.

Raw MS/MS spectra were processed using ProteinLynx Global Server (Waters) and were searched against the IPI murine protein data base by use of the Mascot search algorithm. Full processing and search parameters are given in the supplemental Materials and Methods.

Fibrillization of recPrP—This method follows that previously published (21). Inclusion bodies were isolated from the appropriate bacterial growth as described in the supplemental Materials and Methods.RecPrP was purified by metal ion affinity chromatography, desalted by use of a Hiprep desalting cartridge, and oxidized by the addition of oxidized glutathione overnight. RecPrP was further purified by reverse phase HPLC, and the protein was lyophilized and stored at −20 °C until use. Full details of this procedure are given in the supplemental Materials and Methods.

Recombinant mouse PrP was fibrillized according to the protocol published by Breydo *et al.* (22). Briefly, lyophilized recPrP was dissolved in 6 M guanidine HCl, pH 6.0, at a concentration of 3 mg/ml. A fibrillization reaction consisting of 2 M guanidine HCl, 10 mM thiourea, 120 μg/ml recPrP, 50 mM MES, pH 6.0, and 10 μM thioflavin T was prepared. 160 μl of the reaction mixture was placed into individual wells of a 96-well plate, and 3 Teflon spheres were added to aid mixing. For inclusion of LD9-derived material, proteins from three replicate subcellular fractionations were pooled and resuspended in 800 μl of fibrillization buffer. 200 μl of each subcellular fraction was added to a fibrillization reaction, keeping final concentrations of constituents the same. In some reactions 0.1% (w/w) of preformed recPrP seed was added to the reaction wells. The 96-well plate was incubated at 37 °C with constant shaking (900 rpm, 1-mm diameter). The fluorescence from thioflavin T (ThT) was monitored every 5 min by use of a fluorescence plate reader (Fluoroskan Ascent, Thermo Scientific) with excitation at 444 nm and emission at 485 nm.

Background fluorescence was calculated from four replicate wells containing no recPrP and was subtracted from sample readings. Sigmoidal curves were fitted to the data where possible by a least squares approach. Fluorescence, F, at time, t was calculated from the equation

$$F(t) = A + \frac{(B + ct)}{(1 + e^{(k(t_m - t))})} \quad \text{(Eq. 1)}$$

where A is the initial level of ThT fluorescence, B is the peak level of fluorescence, t_m is the mid point of the transition, and k is the rate of increase of fluorescence. c is an empirical parameter describing changes in fluorescence after fibril formation. The lag time, t_1, is calculated as $t_1 = t_m - 2/k$.

RESULTS

LD9 Cell Homogenates Digest recPrP—The identification of putative co-factors enhancing prion protein misfolding has been a goal of various studies in recent years. To ensure that physiological co-factors are identified, we believe that this can best be achieved through their isolation from defined systems, such as scrapie-susceptible cell lines, and we chose the LD9 fibroblastic cell line for this purpose because these cells have been shown to be susceptible to Chandler-derived strains of scrapie including ME7 and RML (17). LD9 cells were a kind gift of Charles Weissmann (Scripps, Florida). After homogenization of cells, we tested crude homogenates for their ability to enhance the conversion of recPrP in our cell-free conversion assay. Briefly, the assay uses a seed of PrP^{Sc}, isolated from the brains of TSE-infected mice, to catalyze the conformational conversion of recPrP to a PK-resistant isoform. Incorporation of a 3F4 antibody recognition epitope into the recPrP to create the construct Δ3F4-recPrP allows PK-resistant products to be detected specifically against the background of excess murine PrP^{Sc} by standard Western blotting techniques (23). Initial CFCA reactions incorporating crude LD9 cell homogenate yielded an apparent reduction in conversion efficiency relative to control reactions (data not shown). However, Western blot signals corresponding to non-PK-treated recPrP also showed substantial reductions in intensity after CFCA relative to assays containing no cell homogenate, suggesting LD9 homogenate either degrades protein or interferes with its detection. Thus, we tested whether proteases in crude cell homogenates could degrade the recPrP substrate before its conversion in the CFCA. We incubated 20 ng of Δ3F4-recPrP with serial dilutions of LD9 cell homogenate in CFCA buffer without PrP^{Sc} and detected Δ3F4-recPrP by Western blotting. Fig. 1 shows typical results of these experiments. At the highest concentration of cell homogenate tested, no signal corresponding to Δ3F4-recPrP can be seen on the Western blot. After dilution of the homogenate to 1:4000, a signal for Δ3F4-recPrP was restored,

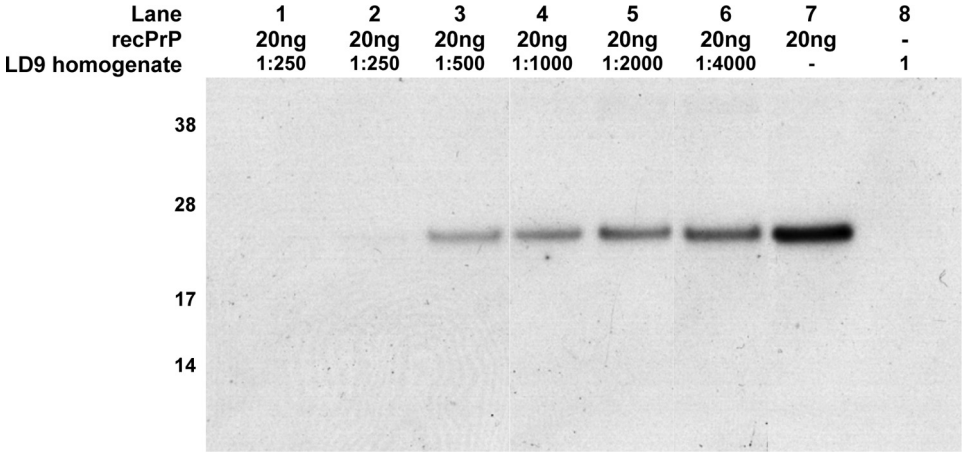

FIGURE 1. **LD9 homogenates digest recombinant PrP.** A Western blot shows the effect of incubation of 20 ng of recPrP with crude LD9 homogenate at various dilutions. *Lanes 7* and *8* contain positive and negative control samples, respectively. 3F4 antibody was used as the antibody for primary detection.

but this remains significantly less than that produced by the control sample. We believe this to be the result of proteases present in the LD9 cell homogenate, which will presumably represent a plethora of different molecules of different specificities and selectivities. The addition of protease inhibitor cocktails to the CFCA is not compatible with subsequent detection of PK-resistant products by treatment with proteinase K; hence, we decided to perform subcellular fractionations to attempt to create fractions that did not have proteases but that may contain conversion-enhancing cofactors.

LD9 Cells Can Be Fractionated by Use of a Continuous Gradient of OptiPrep—Because putative prion cofactors may be protein complexes or may require many molecules from a cellular organelle to allow catalysis of misfolding, we focused on a fractionation regime for LD9 cells that retained organelles as intact as possible. We homogenized flasks of confluent cells in a detergent-free, physiological buffer and fractionated by centrifugation through a gradient of 10–20% OptiPrep. We carefully decanted 500-μl fractions from the top of the tube to produce 22 discrete subcellular fractions. The molecules contained within these fractions were precipitated and resuspended in water, and samples of each fraction were analyzed by SDS-PAGE and Western blotting using antibodies against specific markers of the subcellular organelles of interest.

PrP is a plasma membrane protein and, as such, is expressed in the secretory pathway. Cleavage of N- and C-terminal signal peptides, disulfide bond formation, and post-translational modifications take place in the ER/Golgi body complex, and the mature protein is shuttled to the plasma membrane. PrP is endocytosed from the cell membrane and routed via endosomes for degradation in lysosomes. It has been suggested that conversion of PrP^{C} to PrP^{Sc} takes place on the cell membrane (24) or during transit on the endocytic pathway (25, 26), and we chose markers for both plasma membrane (annexin II) and lysosomes (LAMP-1). We also probed for markers to the ER (BiP) and Golgi body (23C) because the conformational conversion may conceivably take place in these compartments after retrograde translocation (27). Finally, overexpression of PrP^{C} results in its accumulation in mitochondria that leads to neurodegeneration (28). Because this may represent a route of intracellular trafficking of PrP^{C} that occurs under native conditions at undetectable levels but that may be relevant to disease, we also probed for mitochondrial-containing subcellular fractions using Bcl-2 as a marker.

We first demonstrated that each antibody could be used to detect subcellular markers by performing SDS-PAGE separations and Western blotting analyses of crude cell homogenates (supplemental Fig. 1). Subsequently, all 22 subcellular fractions were analyzed for the presence of each marker, and typical Western blots from a subcellular fractionation of LD9 cells are shown in Fig. 2. These data indicate that our OptiPrep gradient successfully separates the various subcellular organelles. Plasma membrane is localized in fractions taken from the top of the gradient, whereas mitochondria are localized toward the bottom of the gradient, as expected based on their known densities. Lysozomes are also located toward the top of the gradient but extend somewhat lower down the gradient than plasma membrane. The markers for Golgi and endoplasmic reticulum are spread across more fractions than the other markers probed, and this is probably the result of partial shearing of these subcellular structures into microsomes during homogenization. Our intention was not to achieve complete purification of any subcellular structures by this method, and the 10–20% OptiPrep gradient provides a useful means of separating LD9 cell homogenates into fractions that are at least enriched for particular organelles before detailed analysis.

Specific Subcellular Fractions from LD9 Cells Enhance Cell-free Conversion of PrP—We tested all subcellular fractions from LD9 cells in our cell-free conversion assay using PrP^{Sc} from ME-7-infected mice as a seed. After each assay we removed a control sample that was not treated with PK, and the amount of conversion can be determined by comparing densitometric signals of bands in PK-treated and untreated samples after Western blotting. For each set of conversion assay reactions, we also did a negative control reaction (without PrP^{Sc}) and a positive control reaction (with PrP^{Sc} but without subcellular fractions).

Representative blots from CFCA experiments incorporating LD9 fractions are shown in Fig. 3. The protein concentration of each fraction was unknown, but equal volumes of each fraction were added to the respective reactions. We found essentially unaltered conversion efficiencies after the addition of fractions from the bottom of the OptiPrep gradient (19–22), and fractions from just above this (14–18) appeared to reduce the conversion efficiency of recPrP slightly. Fractions from in the middle of the gradient, 7-13, resulted in no conversion of recPrP; however, there was also little or no detectable recPrP in lanes that were not treated with PK, suggesting that endogenous LD9 cell proteases were present in these fractions and degraded the recombinant PrP before conversion could take place. However, fractions from the top of the OptiPrep gradient showed clear

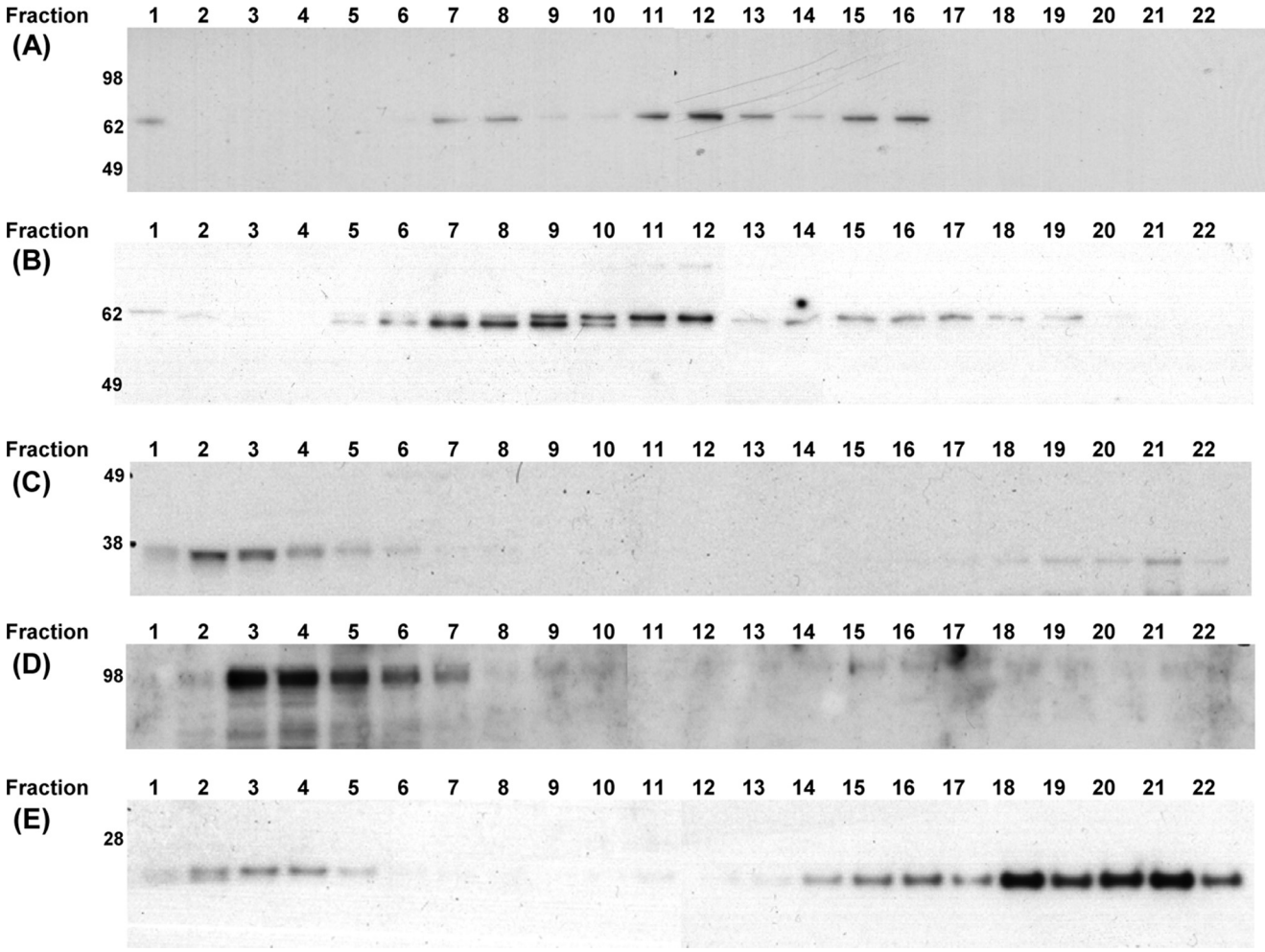

FIGURE 2. **Representative Western blots are shown for subcellular markers in fractions derived from centrifugation fraction of LD9 homogenates through an OptiPrep gradient.** Western blots are using antibodies specific for BiP (*A*), 23C (*B*), annexin II (*C*), LAMP-2 (*D*), and Bcl-2 (*E*).

signs of increased conversion of recombinant PrP, as determined by densitometry of Western blot intensities; compare, for example, *lanes 4* and *7* on Fig. 3, *panel A*. These results indicate that TSE disease-specific co-factors may be present in low density subcellular fractions of LD9 cells.

We performed multiple subcellular fractionations of LD9 cells and carried out repeat CFCA reactions supplemented with each fraction seeded with ME7 PrP^{Sc}. For fractions 7–13, which we previously showed resulted in degradation of the recombinant PrP substrate, we first diluted the fraction from the OptiPrep gradient by 1000-fold, and typical CFCA Western blots for these experiments are shown in Fig. 4, *A* and *B*. These fractions do not enhance recPrP conversion at 1000-fold dilution. We chose this dilution because crude homogenates required dilution of around 1000-fold to prevent excessive degradation of the recPrP substrate during our initial experiments (see Fig. 1). However, we also investigated the effect of dilution of fractions 2, 3, and 4 during conversion assays and found that the enhancing effect was lost after a 200-fold dilution. Thus, although experiments involving fractions 7–13 represent extreme dilutions and one would expect the effect of co-factors to also be diluted, these experiments enable us to say that co-factors are not likely to be present in fractions 7–13 above the level that they are present in fractions 1–5.

After densitometric determination of the percentage of recombinant PrP converted in each reaction and normalization of data, by setting the amount of converted protein in the positive control reaction to represent 100% conversion, we averaged the conversion efficiencies, and the results are shown graphically in Fig. 4*C*; the *error bars* represent ± S.D. Although fractions 7–13 were substantially diluted before the addition in the CFCA and data from these reactions cannot be compared directly with those from other fractions, these have been included on the same graph for illustrative purposes. From additional subcellular fractionations, we blotted for the five markers for subcellular organelles in several replicates and averaged the densitometric intensity of the markers in each fraction, expressing this as a percentage of the total of each marker from each fractionation. These data are also displayed schematically in Fig. 4*C*. The top-most five fractions from the OptiPrep subcellular fractionation enhance the conversion efficiency of recombinant PrP seeded with ME7 PrP^{Sc}; on average, fraction two approximately doubles the conversion efficiency. Between fractions 6–15 there appears to be some inhibition of conversion, perhaps still through partial degradation of the recombinant PrP substrate. Fractions from the bottom of the gradient have no significant effect on conversion. By comparison with relative quantities of markers for subcellular

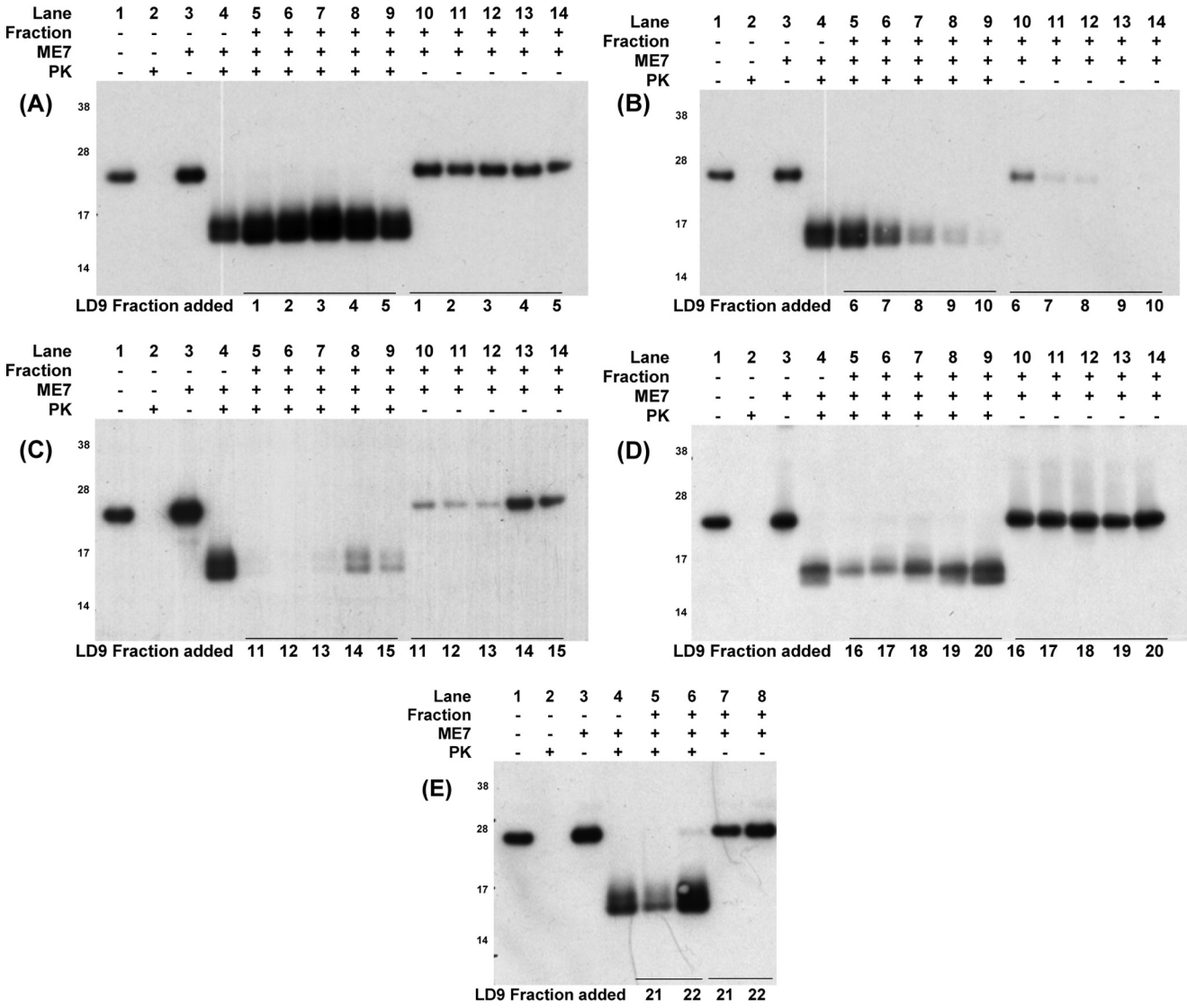

FIGURE 3. **Shown are representative Western blots of the effect of LD9 subcellular fractions on the conversion of Δ3F4-recPrP seeded with PrP^{Sc} derived from ME7-infected mouse brains.** *Panels A–E* show the addition of sequential subcellular fractions from OptiPrep gradients to the cell free conversion assay along with negative controls (*lanes 1* and *2*) and positive controls (*lanes 3* and *4*). For the CFCA reaction, samples without and with proteinase K treatment are included on the Western blot. The densitometric intensity of the *+PK lane* (19/20th of the sample) is compared with the intensity of the respective *−PK* lane (1/20th of the sample) to yield % conversion.

organelles, it can be seen that the conversion efficiencies closely mirror the abundance of annexin II, the plasma membrane marker. These data suggest that CFCA-enhancing co-factors may be present in the plasma membrane or other low-density organelles.

To discount any interfering effects on our CFCA of endogenous PrP^C that are present in the LD9 cell lines, we determined its subcellular location by Western blotting using 8H4 antibody (supplemental Fig. 2*A*). We found that LD9-PrP^C was present in almost all subcellular fractions, a finding that is in agreement with studies on the cell biology of PrP which indicate that at different stages of its cell cycle it is present in ER, Golgi, plasma membrane, and endosomes/lysosomes. By densitometry, we could show that the levels of LD9-PrP^C from each fraction present in the CFCA reactions were negligible compared with the exogenously added recombinant PrP. We conclude that endogenous LD9 PrP^C is unlikely to contribute either positively or negatively to conversion of recombinant PrP, although we cannot rule out that certain forms of PrP at different stages of the molecule life cycle may exert more potent stimulatory or inhibitory effects on recPrP conversion than others.

Conversion Enhancing Fractions Are Composed of Plasmamembrane and Cytoplasmic Proteins—To confirm the identities of proteins present in conversion-enhancing fractions, we subjected fraction 3 from a subcellular fractionation of LD9 cells to mass spectrometric analysis. Proteins were reduced and alkylated with dithiothreitol and iodoacetamide, respectively, and were digested by the addition of trypsin. The tryptic peptides were analyzed by online capillary HPLC-MS/MS, and MS/MS spectra were searched against a non-redundant data base using the Mascot search algorithm. Proteins identified above the significance threshold and for which at least two peptides were identified and with Mascot scores of >200 are listed in Table 1. The Mascot

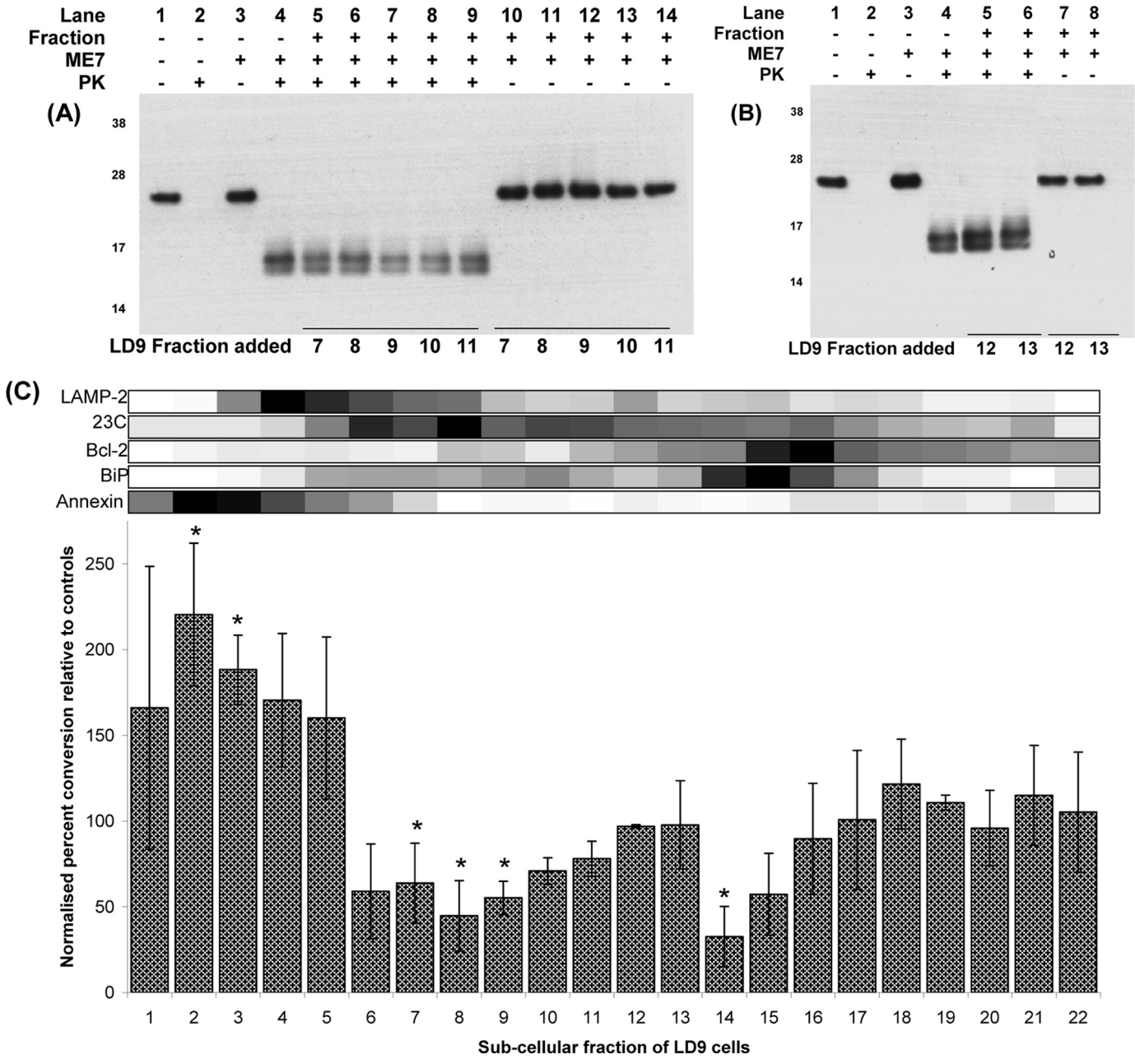

FIGURE 4. *A*, and *B*, shown are representative Western blots of the effect of LD9 subcellular fractions 7–13 at a 1:1000 dilution on the conversion of Δ3F4-recPrP seeded with PrP^{Sc} derived from ME7-infected mouse brains. The densitometric intensity of the *+PK lane* (19/20th of the sample) is compared with the intensity of the respective *−PK lane* (1/20th of the sample) to yield % conversion. *C*, *bar chart* and color heat map showing averaged conversion efficiency in the presence of subcellular fractions ($n = 4$, *error bars* are ± S.D.; * indicates results that are statistically significantly different from controls by Student's *t* test ($p < 0.05$)) along with the averaged abundance of subcellular markers in each fraction (n> = 3).

output can be accessed in the supplemental Materials and Methods. From the Uniprot and Ingenuity knowledge bases, we extracted known and predicted subcellular localization information. The majority of proteins identified were cytoplasmic, and this is in agreement with the presence of proteins that are not contained within discrete organelles in the upper fractions of the gradient. However, we also detected a number of plasma membrane-specific proteins in this fraction. The low efficiency of detection of plasma-membrane proteins by MS approaches is well known, and the overwhelming bias of cytoplasmic proteins detected in fraction 3 over membrane proteins may reflect the poor detection of such proteins by MS. Nevertheless, fractions from the upper portion of the OptiPrep gradient clearly contain both cytoplasmic and plasma membrane proteins.

Buoyant Fractions from Another Scrapie-susceptible Cell Line also Enhance PrP Conversion—We wanted to investigate whether the enhancement of conversion by buoyant LD9 subcellular fractions was a property only of this cell line or whether similar fractions from other TSE-susceptible cell lines would also enhance conversion. For this purpose we cultured scrapie mouse brain (SMB-PS) cells obtained from the TSE Resource Centre. This cell line was originally grown *ex vivo* from the brain of a mouse infected with scrapie and was subsequently

TABLE 1

List of proteins identified as present in fraction 3 from subcellular fractionation of LD9 cells

Proteins were reduced, alkylated, and digested with trypsin, and the resulting peptides were analyzed by online HPLC-MS/MS. Peptide MS/MS data was searched against the ISI Mouse database using the Mascot search algorithm. Proteins with greater than two peptide hits and Mascot Mowse scores greater than 200 are reported here. Full results are given in the supplemental "Materials and Methods." PM, plasma membrane.

Gene name	Protein name	Peptide hits	Mascot protein score	Primary cellular location
Actb	Actin, various forms	3–26	179–3121	Cytoplasm
Tubb5	Tubulin, various forms	5–18	112–1493	Cytoplasm
Hspa8	Heat shock cognate 71-kDa protein	19	1172	Cytoplasm
Eno1	α-Enolase	13	845	Cytoplasm/PM
Hsp90ab1	Heat shock protein 90-kDa β (cytosolic)	20	838	Cytoplasm
Tpi1	Triosephosphate isomerase 1	8	596	Cytoplasm
Ppia	Peptidyl-prolyl cis-trans isomerase	7	555	Cytoplasm
Prdx6	Peroxiredoxin-6	4	549	Cytoplasm/lysosome
Got1	Aspartate aminotransferase, cytoplasmic	5	537	Cytoplasm
Anxa5	Annexin A5	5	511	PM
Gapdh	Glyceraldehyde-3-phosphate dehydrogenase	5	474	Cytoplasm/PM
Pgam1	Phosphoglycerate mutase 1	5	461	Cytoplasm
Ywhaz	14-3-3 protein ζ/δ	7	444	Cytoplasm
Arhgdia	Rho GDP-dissociation inhibitor 1	6	403	Cytoplasm
Pgk1	Phosphoglycerate kinase 1	6	390	Cytoplasm
Gdi2	Isoform 1 of Rab GDP dissociation inhibitor β	4	365	Cytoplasm/PM
Hsp90aa1	Heat shock protein HSP 90α	12	356	Cytoplasm
Ywhab	Isoform Long of 14-3-3 protein β/α	4	352	Cytoplasm
Ywhaq	Isoform 1 of 14-3-3 protein θ	3	337	Cytoplasm
Gsn	Isoform 1 of Gelsolin	5	307	Extracellular space
Eif4b	Eukaryotic translation initiation factor 4B	2	303	Cytoplasm
Lgals1	Galectin-1	6	273	Extracellular space
Cfl1	Cofilin 1	3	264	Cytoplasm/nucleus
Phgdh	D-3-Phosphoglycerate dehydrogenase	6	255	Cytoplasm
Akr1b3	Aldose reductase	4	248	Cytoplasm
Nme2	Nucleoside diphosphate kinase B	4	246	Nucleus
Fdps	Farnesyl pyrophosphate synthetase	4	233	Cytoplasm
Anxa1	Annexin A1	3	231	PM
Ywhag	14-3-3 Protein γ	2	221	Cytoplasm
Eif4a1	Eukaryotic initiation factor 4A-I	4	221	Cytoplasm
Gstm1	Glutathione *S*-transferase μ1	4	218	Cytoplasm
Uap1l1	Isoform 1 of UDP-*N*-acetylhexosamine pyrophosphorylase-like protein 1	3	212	Unknown
Gsto1	Glutathione *S*-transferase ω1	3	209	Cytoplasm
Eno3	β-Enolase	3	202	Cytoplasm
Pebp1	Phosphatidylethanolamine-binding protein 1	2	202	Cytoplasm

cured of TSE infection by treatment with pentosan polysulfate (29). The cured cell line has been shown to be susceptible to multiple mouse-passaged scrapie strains, although not all strains lead to a stable infection.

Using an identical OptiPrep gradient to that used previously, we fractionated homogenates of SMB-PS cells and blotted for the five markers for ER, Golgi body, plasma membrane, lysosomes, and mitochondria. We found tighter distributions of both ER and Golgi markers in SMB cell gradient fractions compared with LD9 cells, and markers for mitochondria and lysosomes showed a similar distribution to those found for LD9 fractionations (supplemental Fig. 3). In addition, annexin II, the plasma membrane marker, was found in the top-most fractions of SMB cell gradients. We also found that SMB-PS cells contained negligible levels of endogenous PrP^{C} compared with the amount of recPrP added to the CFCA reactions (supplemental Fig. 2*B*).

We incubated SMB-PS subcellular fractions in CFCA reactions seeded with ME7. To reduce the significant amount of PrP^{Sc} used in such experiments, we focused only on the top five fractions from the gradient, the equivalent to those LD9 fractions that enhanced conversion. Fig. 5*A* shows a typical Western blot from these experiments. We repeated the subcellular fractionation and the CFCA several times, and the average effect on conversion of recombinant PrP of each fraction was calculated. Normalized conversion efficiencies relative to CFCA reactions in which no subcellular fractions were added for the five upper fractions of the gradient are shown graphically in Fig. 5*B* and are ±S.D. We found that the top-most fractions of SMB-PS cell gradient fractionations also significantly enhanced conversion of recombinant PrP using ME7 PrP^{Sc} as seed. These data indicate that this phenomenon is not cell line-specific, thereby suggesting that conversion-enhancing co-factors are present in various cell lines. Whether cell lines that are incapable of sustaining TSE infections also possess conversion-enhancing co-factors remains to be determined.

LD9 Fractions Enhance Conversion of PrP Seeded with a Different TSE Strain—We also asked whether any co-factors present in LD9 cells were TSE strain-specific. We performed additional fractionations of LD9 cells and incubated them in CFCA reactions seeded with PrP^{Sc} purified from the brains of mice infected with the 79A strain of mouse-passaged scrapie. Conversion using 79A as a seed is inefficient, and average percentage conversion of positive controls were an order of magnitude less than for ME7-seeded conversion assays. As a result, variations in conversion efficiency caused by experimental differences were correspondingly larger, making it difficult to interpret the effect of addition of LD9 subcellular fractions. Nevertheless, we carried out two repeats of CFCA reactions including only fractions 2–4 from LD9 subcellular gradients as sources of co-factors, and we averaged the conversion efficiencies. A typical Western blot from these experiments is shown in Fig. 6*A*, and averaged conversion efficiencies are plotted graph-

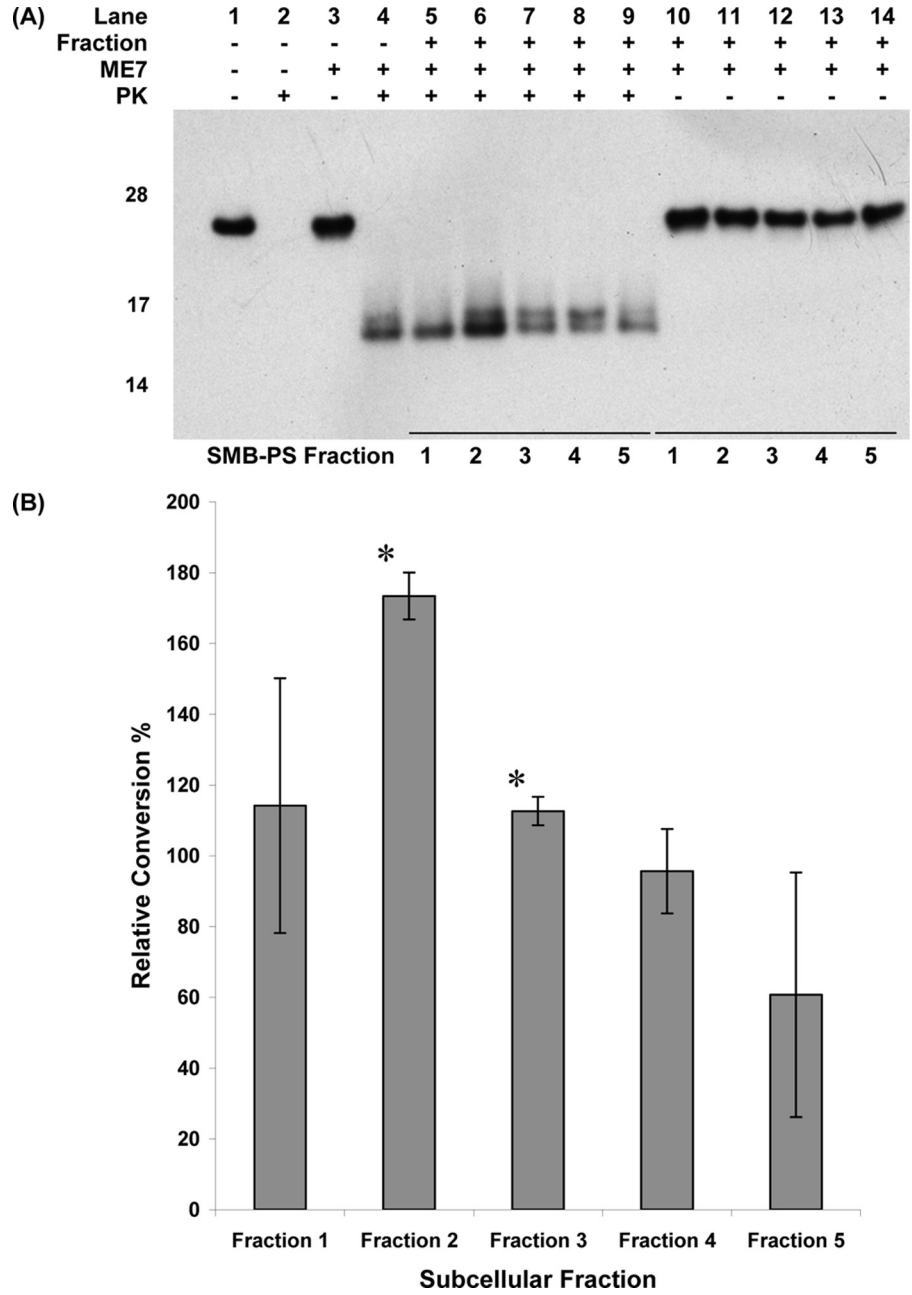

FIGURE 5. *A*, shown are Western blots of the effect of SMB-PS subcellular fractions 1–5 on the conversion of Δ3F4-recPrP seeded with PrP^{Sc} derived from ME7-infected mouse brains. *B*, shown is a *bar chart* of average conversion efficiency of Δ3F4-recPrP seeded with ME7 in the presence of SMB-PS subcellular fractions 1–5. $n = 3$. *Error bars* are ± S.D.; * indicates results that are statistically significantly different from controls by Student's *t* test ($p < 0.05$).

ically in Fig. 6*B*. Although differences in relative conversion efficiency are not statistically significant, the data appear to show that low density LD9 cell fractions also enhance conversion of recombinant PrP seeded with 79A. These results indicate either that co-factors contained in LD9 cells are not TSE strain-specific or that LD9 cells possess different sets of co-factors capable of enhancing conversion by different strains of TSE disease.

LD9 Subcellular Fractions That Enhance Cell-free Conversion Inhibit in Vitro Fibrillization of PrP from Two Different Species—Finally, we hypothesized that cofactors that enhance PrP conversion seeded with exogenous PrP^{Sc} may also catalyze the general misfolding of PrP in alternate *in vitro* reactions. We fibrillized murine PrP by continuous shaking (22) in the presence or absence of the 22 LD9 subcellular fractions, monitoring fibril formation by the increase in ThT fluorescence. In the first experiment we performed four repeat fibrillizations of each sample and fitted sigmoidal curves to the data by least squares approaches to allow measures of fibrillization lag times to be derived. Fig. 7, *panels A–D*, show repeat fibrillizations from samples containing fractions 1, 2, 3, or 8. Fibrillization of murine PrP in the presence of fraction 1 is not significantly different from control fibrillizations (shown in supplemental Fig. 4). However, in the presence of fraction 2, the lag time for fibrillization is extended to the point where fibrillization is only just beginning to occur at the end of the assay period (24 h). No fibrillization is evident in samples containing LD9 fractions 3 or 4, whereas samples containing fraction 5 just begin to fibrillize within the assay time frame again. The addition of fractions 6 and 7 produce fibrillization profiles that are essentially complete within the time scale of the experiment but have significantly longer lag times than control fibrillizations, whereas the addition of fraction 8 yields fibrillization curves that are not significantly different from controls. We confirmed that the rise in ThT fluorescence does indeed correlate to the formation of fibrils by confirming the presence of a PK-resistant product after maturation of fibrils, according to the protocol by Breydo *et al.* (22) (supplemental Fig. 5). Thus, low density fractions that enhance PrP^{Sc}-seeded conversion of recPrP also inhibit *in vitro* fibrillization of the same protein.

Fibrillization is believed to occur exponentially after creation of an initial nucleation complex. To determine whether low density LD9 fractions slowed nucleation of a seed or whether elongation of fibrils after nucleation was slowed, we performed a second set of fibrillization experiments where we added preformed fibrils to half of the samples before fibrillization. In control fibrillization assays without added LD9 fractions, the presence of preformed fibrils shortened lag times dramatically. In the presence of LD9 fractions, lag times to fibrillization of

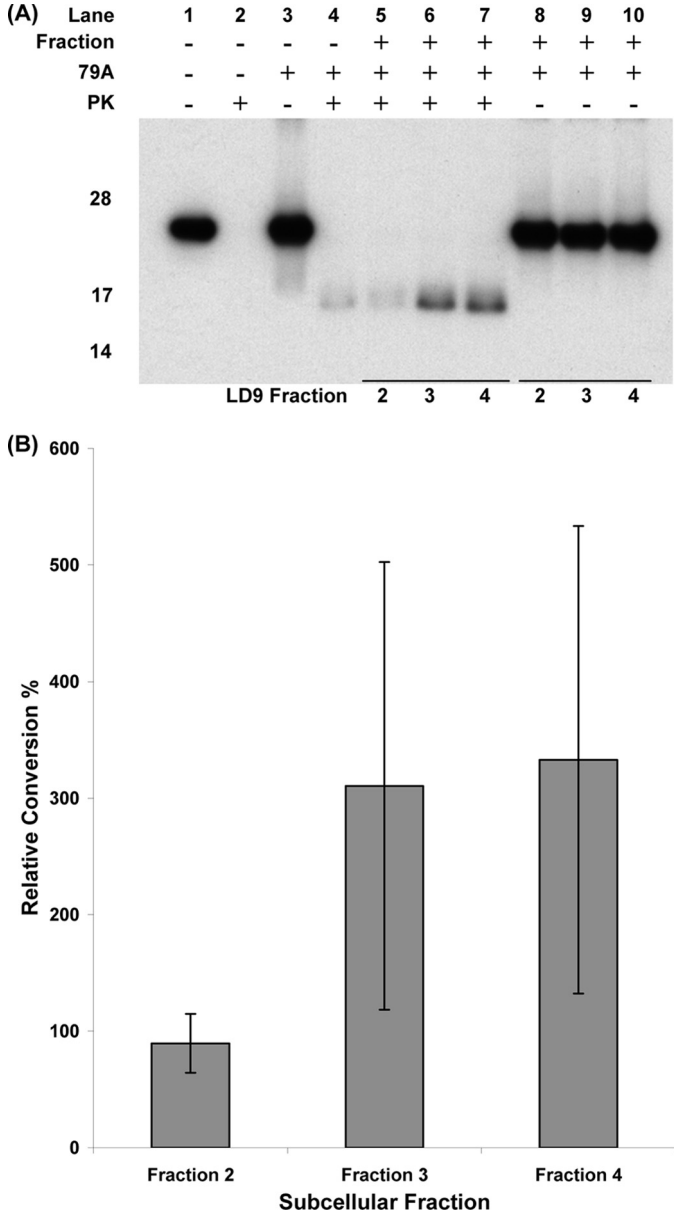

FIGURE 6. *A*, shown are Western blots of the effect of LD9 subcellular fractions 2–4 on the conversion of Δ3F4-recPrP seeded with PrP^{Sc} derived from 79A-infected mouse brains. *B*, shown is a *bar chart* of average conversion efficiency of Δ3F4-recPrP seeded with 79A in the presence of LD9 subcellular fractions 2–4. *Error bars* are ± S.D.; $n = 2$.

seeded assays were always shorter than unseeded assays. However, for fractions that completely abrogated fibrillization of unseeded assays, the addition of preformed seed caused fibrillization to proceed but at a substantially reduced rate of fibrillization. Therefore, we conclude that low density LD9 fractions negatively affect both the nucleation and elongation steps of fibrillization.

The full results from all fibrillization experiments using murine PrP are given in supplemental Fig. 4, from which average lag times of both seeded and unseeded reactions were calculated. For fractions 2, 3, and 4, lag times could not be calculated because sigmoidal curves could not be fit to partial fibrillization data with accuracy. The lag times are presented graphically in Fig. 7*E*, and it can clearly be seen that fractions which enhance CFCA-specific conversion of recPrP also inhibit both seeded and unseeded fibrillization of murine PrP. For fractions 5, 6, and 7, the lag time differences relative to control samples are statistically significant, as determined by Student's *t* test. Interestingly, unseeded reactions incorporating fractions 10 and 11 are also significantly different from controls ($p < 0.05$), but the corresponding seeded reactions are not significantly different. We are currently unsure of the cause of this difference but are undertaking experiments to confirm these results.

DISCUSSION

Various *in vitro* assays have been developed to allow the study of prion protein conformational change, and some assays replicate aspects of TSE disease. The original cell free conversion assay was pioneered by the group of Caughey and co-workers (16) in the 1990s. The assay included radiolabeled recPrP derived from tissue culture as a substrate, and we subsequently modified this assay to use radiolabeled PrP derived from recombinant bacteria (15). Our CFCA has been shown to replicate many aspects of TSE disease, including reduced conversion across species barriers, the effect of amino acid changes in the PrP protein on conversion, and inhibition of conversion by known anti-TSE drugs (30). Conversion efficiencies in this assay are low, however, and there is a need to include an excess of seed over substrate to drive conversion. The low conversion efficiency is in line with the exceptionally long incubation times associated with TSE disease. Of crucial importance is that the output from the CFCA is a measure of the efficiency of the conversion of the substrate; thus, changes in conversion efficiency that result from alterations to assay conditions can be quantified.[6]

More recently, two additional assays have been developed that use the same basic principle as the CFCA but include additional factors resulting in dramatically increased levels of conversion. The PMCA assay uses brain homogenate from scrapie-infected animals to seed conversion of native PrP^{C} contained in brain homogenate from uninfected animals (5). The assay also incorporates sequential rounds of sonication, incubation, and dilution of the assay constituents into uninfected brain homogenate to dilute out the starting seed and to replenish the substrate. A similar assay, termed quaking induced conversion, uses PrP from recombinant bacteria as a substrate and intermittent shaking to drive conversion (12). Like the PMCA assay, sequential rounds of dilution into fresh substrate can dilute out the starting PrP^{Sc}, but the protease-resistant recombinant protein produced has not been shown to be infectious. Thus, although the quaking-induced conversion assay appears to produce PK-resistant recombinant protein when it is seeded with PrP^{Sc}, this may not represent a disease-specific misfolding of recombinant PrP but, rather, a fibrillization catalyzed by the presence of pre-aggregated protein. Crucially, it has also been shown that continual shaking of recombinant PrP alone eventually produces amyloid fibrils that resemble PrP^{Sc} (32), which caused disease in transgenic mice overexpressing PrP (13).

[6] Kirby, L., Agarwal, S., Graham, J., Goldmann, W., and Gill, A. C. (2010) *Biochemistry* **49,** 1448–1459.

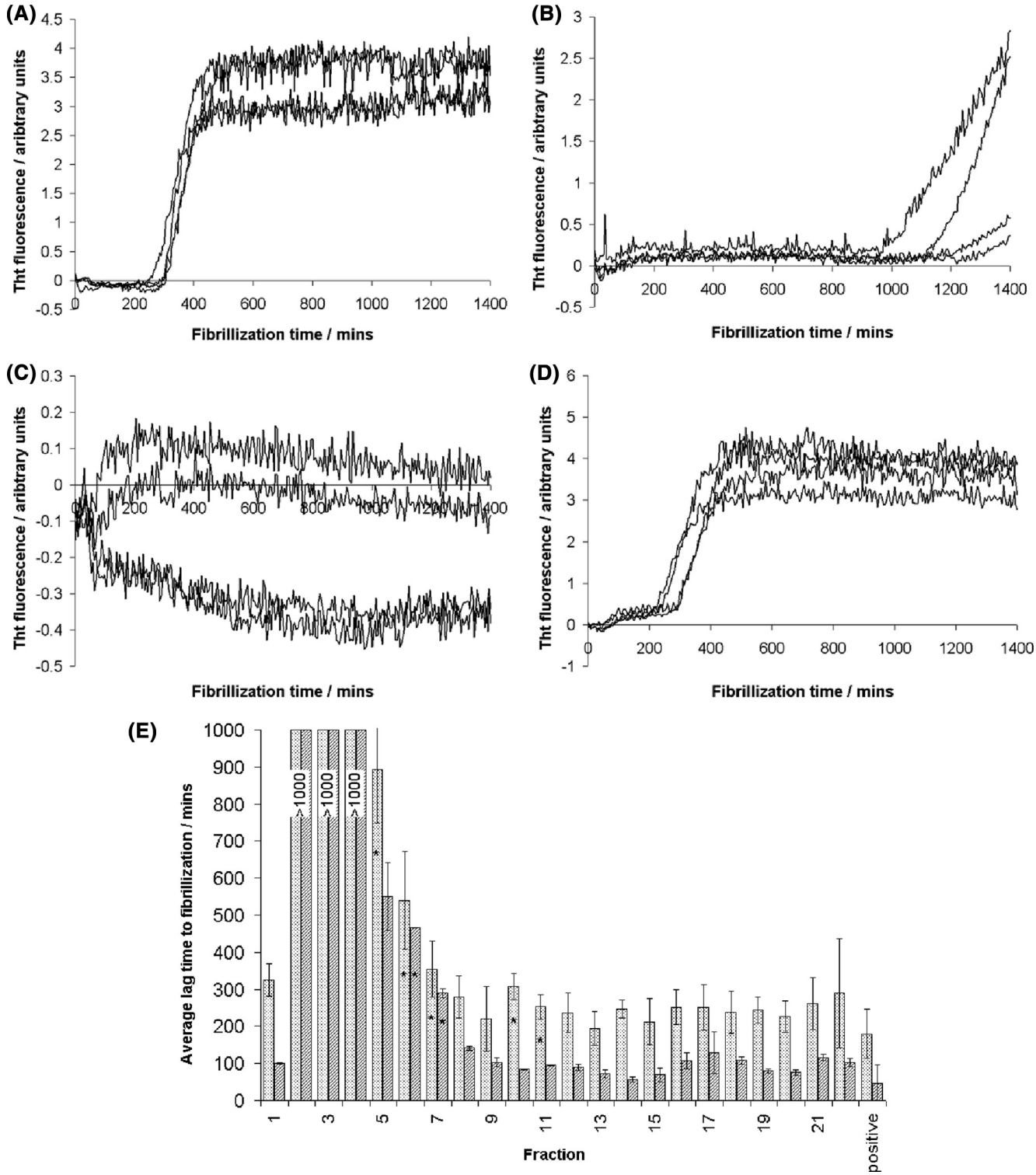

FIGURE 7. *Panels A–D* show graphs of ThT fluorescence as a function of time during fibrillization of recPrP in the presence of LD9 fraction 1 (*A*), LD9 fraction 2 (*B*), LD9 fraction 3 (*C*), and LD9 fraction 8 (*D*). *E*, shown is a *bar chart* showing average lag times to fibrillization of recPrP in the presence of LD9 fractions. *Dotted bars* represent lag times of reactions that were not seeded with preformed fibrils, and *striped bars* represent reactions that were seeded with 0.1% (w/w) preformed fibrils. *Error bars* are ± S.D.; $n = 6$ for unseeded and 2 for seeded reactions. An *asterisk* indicates lag times that are significantly different relative to control reactions with no LD9 fraction added. Lag times for reactions involving fractions 2–4 could not be calculated because no fibrillization was evident in the time scale of the experiment.

Both CFCA and quaking-induced conversion assays use recombinant protein as a substrate and differ from the PMCA assay in that normal brain homogenate is added to this assay as the source of PrP^C substrate. The addition of brain homogenate presumably allows the generation not only of PK-resistant protein but also of TSE infectivity, a disease-specific process. These observations strongly suggest the presence of co-factors present in brain that promote disease-specific folding of PrP, which

results in the generation of *de novo* infectivity. Identification of these factors would increase our understanding of TSE diseases immeasurably, and in our current experiments we have isolated specific low density, subcellular fractions that cause an increase in conversion efficiency of recPrP in our CFCA. Our CFCA does not use shaking, sonication, or other exogenous sources of energy; thus, we suggest that the observed increase in conversion efficiency may be a physiological process. Those fractions that stimulated disease-specific conversion of recPrP came from the upper (low density) regions of the centrifugal gradient; Western blotting for subcellular markers showed this region to contain the plasma membrane marker annexin II, and there was partial overlap with the lysosomal marker, LAMP2. The conversion-enhancing fractions were distinct from those containing markers for Golgi body, ER, or mitochondria, implying that these organelles do not contain prion co-factors.

To confirm that conversion-enhancing fractions contained plasma membrane proteins, we analyzed one such fraction by proteomic techniques and identified 42 different proteins that are contained within this fraction. The majority of these proteins are localized predominately in the cytoplasm, but a handful of plasma membrane-specific proteins were also identified. Mass spectrometric techniques for protein identification are known to under-represent membrane proteins because their hydrophobic nature makes analysis problematic, and it is not clear whether the relative numbers of cytoplasmic *versus* plasma membrane proteins identified are a true representation of the contents of this fraction. From our list of proteins it is tempting to speculate on the involvement of particular proteins in conversion. Certainly, various heat shock proteins were identified in LD9 fraction 3, and the enhancement of conversion of recPrP by molecular chaperones has previously been documented (33). In yeast, heat shock proteins are of crucial importance in mediating the prion phenotypes (34–36) and may also mediate aggregation of various mammalian proteins (37). Additionally, cytoskeletal proteins present in LD9 fraction 3 may create a scaffold that helps catalyze the conformational change of PrP leading to aggresome formation. This mechanism of prion formation has also been suggested in yeast (38), and there is some evidence for aggresome formation in mammalian TSEs (39). However, presently we do not know which, if any, of the identified proteins is the active component, and future work will involve subfractionation of active fractions. We also note that plasma membrane proteins are likely to be isolated from OptiPrep gradients in the presence of small sections of the membrane, thereby co-purifying with various lipids and potentially glycosaminoglycans. We have not tested our active fractions for either class of molecule, but if present, either may have effects on conversion. Both glycosaminoglycans (40–42) and lipids (43–45) have previously been suggested as potential prion cofactors. In addition, Deleault's minimal constituents for prion replication by PMCA (14) includes lipids that co-purify with the PrP^C substrate and poly(A)RNA, which is a polyanionic compound and which may take the place of glycosaminoglycans *in vitro*. Heparin sulfate as well as other polyanionic compounds has also been shown to be an effective catalyst for prion misfolding in the PMCA assay (31). It is possible that our low density fractions contain similar constituents to those suggested by Deleault, but at this stage a thorough analysis of the chemical composition of these fractions is not useful as a wide variety of different molecules may be present within active fractions; further fractionation will allow us to segregate those molecules that participate in conversion from those that happen to co-isolate with them.

To test the specificity of our findings, we performed experiments with PrP^{Sc} from another source of mouse scrapie as seed and also used an additional scrapie-susceptible cell line to provide the source of subcellular fractions. In both cases we found that low density fractions enhanced conversion. At face value, this result implies a certain lack of specificity of the putative cofactors contained in our low density fractions. SMB-PS cells are not susceptible to stable infection with ME7 scrapie, but transient infection can occur,[7] and LD9 cells have not been reported to be infected by 79A scrapie (17). Thus, one might not expect SMB-PS cells to possess co-factors that can cause conversion of recPrP seeded by ME7, and LD9 cell co-factors may not catalyze misfolding seeded with 79A. However, we still know little about why particular cell lines are susceptible to scrapie infection, whereas others are not (8). It is possible that all cells, regardless of origin, are capable of converting PrP^C to a variety of different isoforms but that certain cell lines clear particular isoforms of PrP^{Sc} more readily than others, preventing stable infection with specific TSE strains. Our results suggest that a variety of different cell lines would also be able to supply low density fractions that enhance conversion; in effect, we may be creating a cell-free environment highly amenable to prion misfolding but which contains the necessary molecules for efficient conversion of recPrP in the absence of molecules for efficient removal of PrP^{Sc}.

To test the possibility that conversion-enhancing fractions created optimal conditions for prion misfolding, we used a fibrillization assay to monitor the effect of subcellular fractions on PrP folding in the absence of a PrP^{Sc} seed (22). Our findings are unexpected and indicate that the same fractions that enhance disease-specific misfolding of recPrP also inhibit *in vitro* fibrillization. When the fibrillization was seeded with preformed fibrils of recombinant PrP, produced previously by shaking-induced fibrillization, the lag times of fibrillization in the presence of low density LD9 fibrils were shortened, but fibrillization did not go to completion in the time scale of the assay. Thus, low density LD9 fractions inhibit both initial seed formation and fibril elongation. It is difficult to interpret these results mechanistically, as detailed molecular mechanisms of seeded CFCA and unseeded fibrillization reactions are not known. However, we have recently analyzed the effects of prion protein polymorphisms on both assays and found several polymorphisms that inhibited recPrP conversion in the CFCA yet enhanced oligomerization of the same protein.[6] We found significant differences between stability of the recPrP variants used in these experiments, which correlated with the effects on disease-specific and non-disease specific misfolding. Because our previous data are essentially the reverse of those outlined herein, we believe that the effect of low density LD9 fractions

[7] R. Hennion, IAH Compton, personal communication.

may be to stabilize the structure of recPrP. It is known that the CFCA requires a well folded substrate for conversion to proceed effectively. *In vitro* fibrillization, on the other hand, proceeds by denaturation of the recPrP by inclusion of chaotropes in the assay buffer.

In summary, we present data demonstrating the production of low density, subcellular fractions from two different scrapie-susceptible cell lines that enhance disease-specific misfolding of recombinant prion protein. The active fractions from one cell line is effective in enhancing conversion when the reaction is seeded with PrP^{Sc} from two different strains of scrapie, and taken together, these data suggest that the ability of TSE strains to infect cells may be governed by differential clearance of prion aggregates rather than a lack of ability of cells to convert endogenous PrP^{C} to particular abnormal isoforms. Furthermore, we find that the low density fractions of LD9 cells that enhance disease-specific conversion inhibit *in vitro* fibrillization of recPrP, suggesting that different mechanisms are involved in each misfolding reaction. The active fractions are composed of, at minimum, plasma membrane and cytoplasmic proteins, and experiments to define further their critical components are ongoing.

Acknowledgments—We thank Dr. Alan Bennett for supplying the plasmid encoding Δ3F4-recPrP, Charles Weissmann for supplying LD9 cells, and the TSE Resource Centre for supplying the SMB-PS cells.

REFERENCES

1. Prusiner, S. B. (1998) *Proc. Natl. Acad. Sci. U.S.A.* **95,** 13363–13383
2. Castilla, J., Morales, R., Saá, P., Barria, M., Gambetti, P., and Soto, C. (2008) *EMBO J.* **27,** 2557–2566
3. Colby, D. W., Giles, K., Legname, G., Wille, H., Baskakov, I. V., DeArmond, S. J., and Prusiner, S. B. (2009) *Proc. Natl. Acad. Sci. U.S.A.* **106,** 20417–20422
4. Makarava, N., Kovacs, G. G., Bocharova, O., Savtchenko, R., Alexeeva, I., Budka, H., Rohwer, R. G., and Baskakov, I. V. (2010) *Acta Neuropathol.* **119,** 177–187
5. Saá, P., Castilla, J., and Soto, C. (2006) *J. Biol. Chem.* **281,** 35245–35252
6. Supattapone, S., Deleault, N. R., and Rees, J. R. (2008) *Methods Mol. Biol.* **459,** 117–130
7. Caughey, B., Raymond, G. J., and Bessen, R. A. (1998) *J. Biol. Chem.* **273,** 32230–32235
8. Weissmann, C. (2009) *Folia Neuropathol.* **47,** 104–113
9. Fasano, C., Campana, V., and Zurzolo, C. (2006) *J. Mol. Neurosci.* **29,** 195–214
10. Geoghegan, J. C., Valdes, P. A., Orem, N. R., Deleault, N. R., Williamson, R. A., Harris, B. T., and Supattapone, S. (2007) *J. Biol. Chem.* **282,** 36341–36353
11. Atarashi, R., Moore, R. A., Sim, V. L., Hughson, A. G., Dorward, D. W., Onwubiko, H. A., Priola, S. A., and Caughey, B. (2007) *Nat. Methods* **4,** 645–650
12. Atarashi, R., Wilham, J. M., Christensen, L., Hughson, A. G., Moore, R. A., Johnson, L. M., Onwubiko, H. A., Priola, S. A., and Caughey, B. (2008) *Nat. Methods* **5,** 211–212
13. Legname, G., Baskakov, I. V., Nguyen, H. O., Riesner, D., Cohen, F. E., DeArmond, S. J., and Prusiner, S. B. (2004) *Science* **305,** 673–676
14. Deleault, N. R., Harris, B. T., Rees, J. R., and Supattapone, S. (2007) *Proc. Natl. Acad. Sci. U.S.A.* **104,** 9741–9746
15. Kirby, L., and Hope, J. (2004) in *Techniques in Prion Research-Methods and Tools in Biosciences and Medicine* (Lehmann, S., and Grassi, J., eds) Birkhauser, Basel, Switzerland
16. Kocisko, D. A., Come, J. H., Priola, S. A., Chesebro, B., Raymond, G. J., Lansbury, P. T., and Caughey, B. (1994) *Nature* **370,** 471–474
17. Mahal, S. P., Baker, C. A., Demczyk, C. A., Smith, E. W., Julius, C., and Weissmann, C. (2007) *Proc. Natl. Acad. Sci. U.S.A.* **104,** 20908–20913
18. Hope, J., Multhaup, G., Reekie, L. J., Kimberlin, R. H., and Beyreuther, K. (1988) *Eur. J. Biochem.* **172,** 271–277
19. Kirby, L., Goldmann, W., Houston, F., Gill, A. C., and Manson, J. C. (2006) *J. Gen. Virol.* **87,** 3747–3751
20. Ritchie, M. A., Gill, A. C., Deery, M. J., and Lilley, K. (2002) *J. Am. Soc. Mass Spectrom.* **13,** 1065–1077
21. Makarava, N., and Baskakov, I. V. (2008) *Methods Mol. Biol.* **459,** 131–143
22. Breydo, L., Makarava, N., and Baskakov, I. V. (2008) *Methods Mol. Biol.* **459,** 105–115
23. Kascsak, R. J., Rubenstein, R., Merz, P. A., Tonna-DeMasi, M., Fersko, R., Carp, R. I., Wisniewski, H. M., and Diringer, H. (1987) *J. Virol.* **61,** 3688–3693
24. Caughey, B., and Raymond, G. J. (1991) *J. Biol. Chem.* **266,** 18217–18223
25. Borchelt, D. R., Taraboulos, A., and Prusiner, S. B. (1992) *J. Biol. Chem.* **267,** 16188–16199
26. Taraboulos, A., Raeber, A. J., Borchelt, D. R., Serban, D., and Prusiner, S. B. (1992) *Mol. Biol. Cell* **3,** 851–863
27. Béranger, F., Mangé, A., Goud, B., and Lehmann, S. (2002) *J. Biol. Chem.* **277,** 38972–38977
28. Hachiya, N. S., Yamada, M., Watanabe, K., Jozuka, A., Ohkubo, T., Sano, K., Takeuchi, Y., Kozuka, Y., Sakasegawa, Y., and Kaneko, K. (2005) *Neurosci. Lett.* **374,** 98–103
29. Birkett, C. R., Hennion, R. M., Bembridge, D. A., Clarke, M. C., Chree, A., Bruce, M. E., and Bostock, C. J. (2001) *EMBO J.* **20,** 3351–3358
30. Kirby, L., Birkett, C. R., Rudyk, H., Gilbert, I. H., and Hope, J. (2003) *J. Gen. Virol.* **84,** 1013–1020
31. Deleault, N. R., Geoghegan, J. C., Nishina, K., Kascsak, R., Williamson, R. A., and Supattapone, S. (2005) *J. Biol. Chem.* **280,** 26873–26879
32. Bocharova, O. V., Breydo, L., Parfenov, A. S., Salnikov, V. V., and Baskakov, I. V. (2005) *J. Mol. Biol.* **346,** 645–659
33. DebBurman, S. K., Raymond, G. J., Caughey, B., and Lindquist, S. (1997) *Proc. Natl. Acad. Sci. U.S.A.* **94,** 13938–13943
34. Grimminger-Marquardt, V., and Lashuel, H. A. (2010) *Biopolymers* **93,** 252–276
35. Masison, D. C., Kirkland, P. A., and Sharma, D. (2009) *Prion* **3,** 65–73
36. Summers, D. W., Douglas, P. M., and Cyr, D. M. (2009) *Prion* **3,** 59–64
37. Arimon, M., Grimminger, V., Sanz, F., and Lashuel, H. A. (2008) *J. Mol. Biol.* **384,** 1157–1173
38. Ganusova, E. E., Ozolins, L. N., Bhagat, S., Newnam, G. P., Wegrzyn, R. D., Sherman, M. Y., and Chernoff, Y. O. (2006) *Mol. Cell. Biol.* **26,** 617–629
39. Kristiansen, M., Messenger, M. J., Klöhn, P. C., Brandner, S., Wadsworth, J. D., Collinge, J., and Tabrizi, S. J. (2005) *J. Biol. Chem.* **280,** 38851–38861
40. Ben-Zaken, O., Tzaban, S., Tal, Y., Horonchik, L., Esko, J. D., Vlodavsky, I., and Taraboulos, A. (2003) *J. Biol. Chem.* **278,** 40041–40049
41. Horonchik, L., Tzaban, S., Ben-Zaken, O., Yedidia, Y., Rouvinski, A., Papy-Garcia, D., Barritault, D., Vlodavsky, I., and Taraboulos, A. (2005) *J. Biol. Chem.* **280,** 17062–17067
42. Wong, C., Xiong, L. W., Horiuchi, M., Raymond, L., Wehrly, K., Chesebro, B., and Caughey, B. (2001) *EMBO J.* **20,** 377–386
43. Critchley, P., Kazlauskaite, J., Eason, R., and Pinheiro, T. J. (2004) *Biochem. Biophys. Res. Commun.* **313,** 559–567
44. Kazlauskaite, J., and Pinheiro, T. J. (2005) *Biochem. Soc. Symp.* **72,** 211–222
45. Kazlauskaite, J., Sanghera, N., Sylvester, I., Vénien-Bryan, C., and Pinheiro, T. J. (2003) *Biochemistry* **42,** 3295–3304